Jahn–Teller effect in $BaTiO_3:Cr^{5+}$: an electron paramagnetic resonance study

2009 J. Phys.: Condens. Matter 21 075904

(http://iopscience.iop.org/0953-8984/21/7/075904)

J. Phys.: Condens. Matter **21** (2009) 075904 (7pp) doi:10.1088/0953-8984/21/7/075904

Jahn–Teller effect in $BaTiO_3$:Cr^{5+}: an electron paramagnetic resonance study

R Böttcher[1,4], H T Langhammer[2] and T Müller[3]

[1] Fakultät für Physik und Geowissenschaften, Universität Leipzig, Linnéstraße 5, D-04103 Leipzig, Germany
[2] Physikalisches Institut, Martin-Luther-Universität Halle-Wittenberg, Friedemann-Bach-Platz 6, D-06108 Halle, Germany
[3] Chemisches Institut, Martin-Luther-Universität Halle-Wittenberg, Kurt-Mothes-Straße 2, D-06120 Halle, Germany

E-mail: boettch@physik.uni-leipzig.de, hans.langhammer@physik.uni-halle.de and thomas.mueller@chemie.uni-halle.de

Received 3 November 2008, in final form 11 December 2008
Published 29 January 2009
Online at stacks.iop.org/JPhysCM/21/075904

Abstract
Electron paramagnetic resonance (EPR) spectra of Cr_I^{5+} defects incorporated on Ti^{4+} sites in single-crystal and powdered ceramics of $BaTiO_3$ were investigated in the temperature range 50–220 K at 34 GHz (Q band). Single-crystal and powder measurements allow the unambiguous determination of the full g tensor in the ferroelectric rhombohedral phase whereas in the orthorhombic phase only the determination of the principal values of the Cr_I^{5+} g tensor was successful. The $T_2 \otimes e$ Jahn–Teller effect stabilizes the vibronic ground state of the $3d^1$ electron of the Cr_I^{5+} ion and leads to a tetragonally compressed defect-O_6 octahedron with the point symmetry D_{4h}. The spontaneous electrical polarization present in the ferroelectric phases of $BaTiO_3$ appears as a further perturbation. The quadratic field effect reduces the D_{4h} symmetry of the Cr_I^{5+} defect centre and produces an additional g tensor breaking the tetragonal symmetry of the Zeeman term. For symmetry reasons one of the principal axes of the rhombic g tensor must be directed along one ⟨110⟩ direction. The angles of the other two principal axes with respect to the ⟨001⟩ axes are dependent on the absolute value of the spontaneous polarization. The difference in the temperature behaviour of the single-crystal and powder spectra can be explained by the presence of internal stress in the grains of the ceramic samples which increases the JT energy of the $3d^1$ electron.

1. Introduction

Barium titanate ($BaTiO_3$) is a material system of fundamental importance for a wide range of technical applications and, due to the variety of phase transitions, a model system of the physical description of ferroelectricity. Besides the well-known, temperature-driven phase transitions (*cubic* $\xrightarrow{398\ K}$ *tetragonal* $\xrightarrow{273\ K}$ *orthorhombic* $\xrightarrow{183\ K}$ *rhombohedral*) of the 3C modification this perovskite shows a further one into the hexagonal high-temperature phase (6H modification) which is stable at temperatures >1703 K in air as far as undoped material is concerned. Defects, particularly 3d and 4d ions, change the physical properties of this material and the technical application is supported by the possibility to tailor its physical properties by purposeful incorporation. During the past several years, extensive electron paramagnetic resonance (EPR), optical and electrical studies have provided a catalogue of the microscopic properties of paramagnetic ions incorporated in $BaTiO_3$. In the case of the Cr^{5+} ion with the $3d^1$ configuration the single-crystal EPR spectra were observed by Possenriede in the low-temperature range for the first time [1]. Two different types of spectra (Cr_I^{5+} and Cr_{II}^{5+}) with rhombic g tensors were detected. An interesting feature of these spectra is the exceptionally large number of magnetically non-equivalent centres and the unexpected directions of principal axes of their g tensors with respect to crystallographic axes.

Possenriede has conjectured that symmetry and g values of the two different Cr^{5+} defects are caused by breaking the

[4] Author to whom any correspondence should be addressed.

symmetry of the T_2 ground state as a consequence of the Jahn–Teller effect (JTE) [1]. However, a microscopic model explaining the somewhat surprising symmetry of the Cr_I^{5+} g tensor does not exist.

Two different EPR spectra of Cr^{5+} ions have also been observed in cubic $SrTiO_3$, which are caused by different impurity sites with either tetragonal or orthorhombic local symmetry [2, 3]. In the presence of uniaxial stress and electrical fields EPR studies of Cr^{5+} with locally tetragonal surroundings confirmed that the octahedral–tetragonal reduction of the site symmetry is caused by $T_2 \otimes e$ static JTE [3, 4]. Müller *et al* discussed that Cr^{5+} with orthorhombic site symmetry corresponds to an off-centre case, in which Cr^{5+} is transformed from an octahedral into a tetrahedral site through a displacement along one of the ⟨110⟩ crystallographic directions so that the ion becomes quasi-tetrahedrally coordinated by four O^{2+} ions [5]. From EPR measurements in the presence of external electric fields the dipole moment associated with the off-centred Cr^{5+} ion and its displacement has been determined [6].

The present study is part of systematic efforts to elucidate the influence of paramagnetic ions and intrinsic defects on the crystal structure of $BaTiO_3$ and to understand their microscopic properties in the 3C and 6H modification in dependence on the defect concentration and parameters of the sintering process of ceramic samples [7–11]. For example, doping with chromium [9, 10], manganese [7], iron [11] and copper [8] decreases the transition temperature cubic–hexagonal and stabilizes the 6H modification at room temperature for distinct threshold concentrations of the dopant.

In this work we investigated Cr-doped $BaTiO_3$ samples in its 3C modification preventing the impurity-induced high-temperature 3C–6H phase transition either by a sufficiently low Cr concentration (single crystal) or by a sufficiently low sintering temperature (ceramic samples). First, we perform single-crystal measurements in the Q band and determine the full g tensors with very high accuracy and, thereafter, the temperature dependences of single-crystal and ceramics powder spectra are investigated. In the rhombohedral phase, the number of branches in the angular dependence and the orientation of the principal axes of the rhombic g tensors are explained under consideration of (1) the Jahn–Teller (JT) distortion of the local surroundings of the Cr_I^{5+} ion, (2) the spontaneous electrical polarization P_s and (3) the domain structure of the samples. The influence of the electrical polarization, however, is expected to be small enough and considered as a weak perturbation of the tetragonal JT distortion. In contrast to the single crystals, the Cr_I^{5+} spectra in the ceramic samples are detectable up to 220 K and thus allow the determination of the principal g tensor values in the orthorhombic phase before line broadening effects make detection of the spectra impossible.

2. Experimental procedure

The $BaTiO_3$ crystals were grown by Albers by the top-seeded solution method [12]. The investigated specimen had dimensions of $1 \times 1 \times 2$ mm^3. The Cr defects were present as unintended background impurities in the nominally undoped multi-domain crystal. The crystal was aligned on a quartz rod so that the rod axis coincided with one of the pseudocubic [001] axes. The spectra were recorded as a function of the direction of the applied magnetic field in the (001) plane.

Ceramic powder with the nominal composition $BaTiO_3 + 0.04BaO + 0.01Cr_2O_3$ was prepared by the conventional mixed-oxide powder technique. After mixing (agate balls, water) and calcining (1373 K, 2 h) of $BaCO_3$ (Solvay, VL600, <0.1 mol% Sr), TiO_2 (Merck, no. 808) and Cr_2O_3 (Merck, p.a.), the $BaTiO_3$ powder was fine-milled (agate balls, 2-propanole) and densified to discs with a diameter of 6 mm and a height of nearly 3 mm. The samples were sintered in air at a temperature of 1350 °C for 1 h (heating rate 10 K min^{-1}). The overall phase composition was checked at room temperature by analysing the XRD powder pattern (STADI MP diffractometer, STOE, Germany). All samples were in the single-phase state (3C modification).

EPR measurements of the single crystal and the finely pulverized ceramics were carried out in the Q band (34 GHz) with a Bruker EMX device. Temperatures between 5 and 240 K were achieved with an Oxford flowing He gas cryostat in connection with an Oxford ITC controller (temperature stability about 0.2 K). More details of the measuring procedure are given in [9]. The spectra of the chromium isotopes without nuclear magnetic moments (^{50,52,54}Cr) are described by an $S = 1/2$ spin-Hamiltonian consisting only of the anisotropic Zeeman term

$$\hat{H} = \beta \vec{B} \underline{\underline{g}} \hat{\vec{S}} \tag{1}$$

with $\underline{\underline{g}}$ the electronic g tensor (symmetric) and β the Bohr magneton, respectively. For the determination of the spin-Hamiltonian parameters and the evaluation of the ceramic powder EPR spectra the MATLAB[5] toolbox for electron paramagnetic resonance 'Easy Spin 2.0.3' was used [13]. By simulating the Q band powder spectra by variation of the parameters of the standard spin-Hamiltonian (1) for the 1/2-spin system Cr^{5+}, a satisfactory accuracy in the determination of the spectral parameters was achieved. The assumption that the spectrum of one defect species in the $BaTiO_3$ powder sample can be modelled by the same g tensor is hardly ever applicable because its local symmetry is distorted by strain effects. For the 1/2-spin Cr^{5+} ion we used a distribution of the principal values of the g tensor in the simulation of the powder spectra. Assuming random fluctuations in the local lattice parameters in the vicinity of the paramagnetic impurity these distributions can be approximated by a Gaussian with the full widths at half-height (FWHH) $\Delta g_1, \Delta g_2$ and Δg_3.

3. Results

3.1. Single-crystal EPR spectra

Figure 1 shows the EPR spectrum of a multi-domain $BaTiO_3$ crystal measured in the rhombohedral phase ($T = 50$ K) at 34 GHz (Q band), the external magnetic field B being parallel to the pseudocubic axis [100]. The three intensive lines

[5] MATLAB is a registered trademark of MathWorks, Inc., Natick, MA, USA.

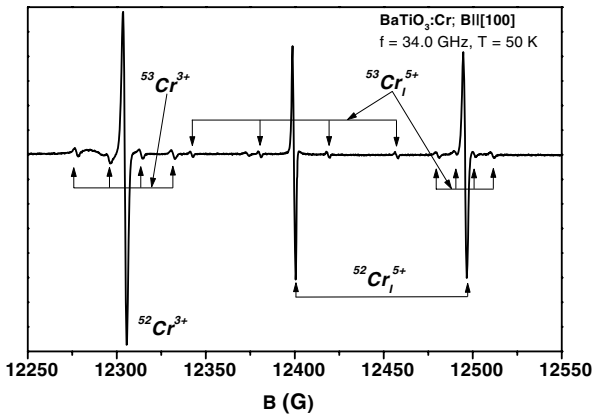

Figure 1. EPR spectrum of a Cr-doped, multi-domain $BaTiO_3$ crystal, measured at 34.0 GHz (Q band) and $T = 50$ K (rhombohedral phase). The magnetic field is parallel to the pseudocubic [100] axis.

must be assigned to chromium impurities on the basis of their satellite structure, caused by hyperfine interaction of the ^{53}Cr isotope (natural abundance about 10%) with the nuclear spin $I = 3/2$. The low-field line belongs to the central transition ($M_S = +1/2 \leftrightarrow M_S = -1/2$) of the Cr^{3+} impurities (Cr^{3+} has the electron spin $S = 3/2$) with trigonal local symmetry. The symmetry axis of its fine structure tensor is directed along one of the eight possible $\langle 111 \rangle$ axes. Because the axial fine structure parameter D is proportional to the square of the electrical polarization of the domain only four sets of Cr^{3+} spectra are observed if the external magnetic field has an arbitrary orientation with respect to the crystallographic axes [12]. For $B \parallel [100]$ the spectra coincide with each other so that only one Cr^{3+} spectrum is detectable. The fine structure transitions ($M_S = \pm 3/2 \leftrightarrow M_S = \pm 1/2$) are broadened by strain effects and their observation is difficult due to their low signal heights.

In figure 1 the other two intensive lines (linewidths ΔB_{pp} about 1.5 G) belong to the Cr_I^{5+} defects which were observed by Possenriede [1] for the first time. Each of them is flanked by hyperfine lines (relative intensity of about 2.5%) caused by $^{53}Cr_I^{5+}$ centres. In our investigation, we confine ourselves to the lines of Cr_I^{5+} ions without nuclear momentum. In figure 2 their angular dependence for a rotation of the single crystal around the pseudocubic axis [001], measured in the Q band (34 GHz) at 50 K, is depicted. If the magnetic field B is lying in an arbitrary orientation in the (001) plane, six lines are observed. In special directions of B the number of lines is reduced: for $B \parallel [100]$ and [110] only two and four lines are observable, respectively. A further splitting of the lines is visible if the magnetic field is not in a pseudocubic plane, and up to 12 lines appear in the spectra. For this reason 12 chemically equivalent Cr_I^{5+} defect centres with the same principal values of the g tensors, but with different principal eigenvectors, must exist in the crystal. In consideration of the domain structure in the rhombohedral phase of $BaTiO_3$ the full g tensors of the 12 defect centres were estimated from the experimental data in the reference system $x \parallel [100]$, $y \parallel [010]$, $z \parallel [001]$ (figure 2). The tensors can be divided into three

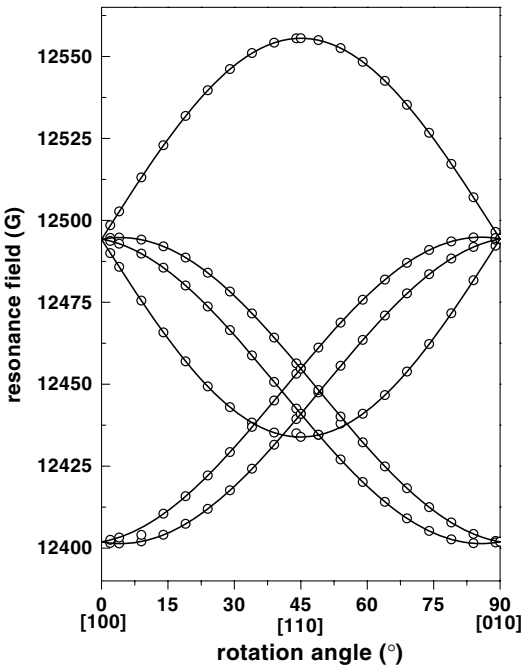

Figure 2. Angular variation of the Cr_I^{5+} lines in the rhombohedral phase (50 K), measured at 34.0 GHz (Q band). Rotation axis is the pseudocubic [001] axis.

Table 1. Principal values and the FWHH of the distributions of the g tensors for the Cr_I^{5+} defects in the rhombohedral (spectral type a, single-crystal, powdered ceramic sample) and orthorhombic (spectral type b, powdered ceramic sample) phase of $BaTiO_3$. The experimental error of the g values for the single-crystal and the powder samples is ± 0.0002 and ± 0.0005, respectively. For FWHH it is ± 0.0002.

Sample	T (K)	g_1	g_2	g_3	Δg_1	Δg_2	Δg_3
Crystal type a	50	1.9351	1.9536	1.9595	—	—	—
Powder type a	50	1.9347	1.9533	1.9596	0.0030	0.0015	0.0007
Powder type a	160	1.9338	1.9529	1.9588	0.0035	0.0017	0.0008
Powder type b	160	1.9394	1.9510	1.9564	0.0040	0.0017	0.0011

groups. The following ones (1–4) belong to the first group:

$$g_{1,2} = \begin{pmatrix} 1.9446 & \pm 0.0095 & 0.0011 \\ \pm 0.0095 & 1.9446 & \pm 0.0011 \\ 0.0011 & \pm 0.0011 & 1.9591 \end{pmatrix}$$

$$g_{3,4} = \begin{pmatrix} 1.9446 & \pm 0.0095 & -0.0011 \\ \pm 0.0095 & 1.9446 & \mp 0.0011 \\ -0.0011 & \mp 0.0011 & 1.9591 \end{pmatrix}.$$

The experimental results show that the elements of the remaining ones are generated by cyclic permutations of the coordinates xyz of tensors 1–4. Their principal values g_1, g_2, and g_3 are given in table 1. Since the simulation of the powder spectrum generates the same principal values, the Schonland ambiguity [14] does not exist.

The principal eigenvector $\vec{e}_1$ of the g_1 tensor is parallel to the $[\bar{1}10]$ direction, the others ($\vec{e}_2$, and $\vec{e}_3$) are lying in the $(\bar{1}10)$ plane. The angle between the vector $\vec{e}_3$ and the [001]

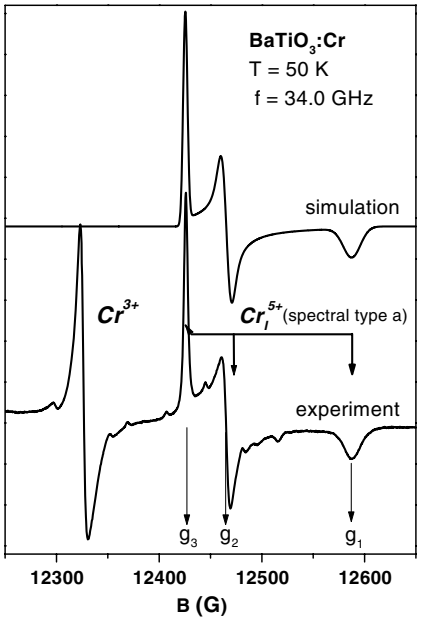

Figure 3. Experimental and simulated EPR powder spectrum (Q band, $T = 50$ K) of the Cr-doped ceramic sample in the rhombohedral phase. In the simulation, only Cr_I^{5+} defect centres without nuclear moments were considered.

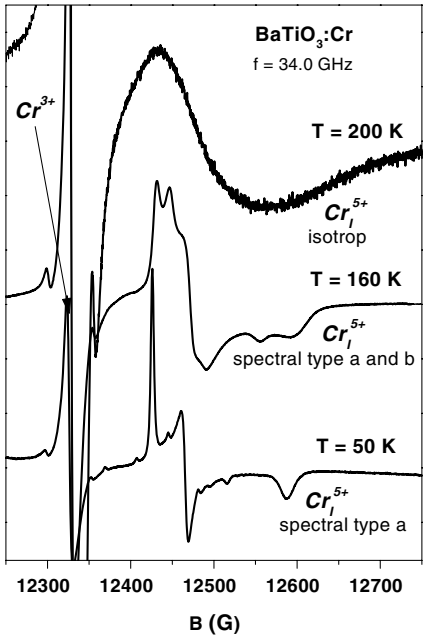

Figure 4. Temperature dependence of the EPR powder spectrum of the Cr-doped ceramic sample measured at 34.0 GHz (Q band).

axis amounts to 15.6°. Rotations around the z axis with the angle $\pi/2, \pi$ and $3\pi/2$ transform the vectors $\vec{e}_1, \vec{e}_2, \vec{e}_3$ into the eigenvectors of tensors 2, 3 and 4, respectively. The eigenvectors of the g tensors in the second and third group are connected with $\vec{e}_1, \vec{e}_2, \vec{e}_3$ of the first group by permutations and rotations around the x or y axes. The principal g values are only weakly temperature-dependent. With increasing temperature the lines of the Cr_I^{5+} defects are broadened: at 110 K the peak-to-peak linewidths ΔB_{pp} are (12 ± 2) G. Above the temperature $T = 120$ K the spectra are no longer detectable in the single crystal.

3.2. Spectra of polycrystalline ceramic powder

The spectrum of polycrystalline Cr-doped $BaTiO_3$ at 50 K is depicted in figure 3 at the bottom. In the low-field part the central peak of the Cr^{3+} spectrum is shown. Its asymmetric shape is caused by the weak angular dependence of the resonance field of the $1/2 \leftrightarrow -1/2$ transition due to the second-order effect. The other peaks belong to the powder spectrum of the Cr_I^{5+} defects (spectral type a) in the rhombohedral phase. The different heights and widths of these peaks are remarkable. The g_1 peak in the high-field part has the largest width. The powder peaks are broadened by g strain effects. The g values and the FWHH of their distribution (given in table 1) were estimated by simulation of the powder spectrum (figure 3, at the top). The g values of spectral type a agree with the single-crystal values. Increasing the temperature, the peaks are broadened and additional peaks appear in the powder pattern above 150 K (figure 4). This new spectrum (type b) can likewise be explained by a simple spin-Hamiltonian (1) with the electron spin $S = 1/2$ and a rhombic g tensor. The spectral parameters are also specified in table 1. On the basis of the experimentally determined g values, this spectrum is assigned to Cr^{5+} defect centres as well. By further increasing the temperature, its intensity increases whereas the centre concentration of the spectral type a diminishes. Furthermore, the widths of all peaks of the spectral types a and b increase. At 200 K only a symmetric line without any structure appears in the spectrum (figure 4). Its intensity is likewise reduced with increasing temperature. Above 220 K only the Cr^{3+} central peak is visible in the powder spectrum.

4. Discussion

Chromium ions are incorporated into the perovskite lattice on the B sites as Cr^{2+} (electron configuration $3d^4$ with the free-ion ground state ^5D), $Cr^{3+}(3d^3, {}^4F)$, $Cr^{4+}(3d^2, {}^3F)$ and/or $Cr^{5+}(3d^1, {}^2D)$. In the high-temperature (paraelectric) phase of these crystals the ions are surrounded by six oxygen ions forming a regular octahedron. Owing to the local electrical crystal field with cubic symmetry the orbital degeneracy of the free-ion states is partially lifted [15]:

$$^5D(Cr^{2+}) \rightarrow {}^5E_g(Cr^{2+}) + {}^5T_{2g}(Cr^{2+})$$

$$^4F(Cr^{3+}) \rightarrow {}^4A_{2g}(Cr^{3+}) + {}^4T_{2g}(Cr^{3+}) + {}^4T_{1g}(Cr^{3+})$$

$$^3F(Cr^{4+}) \rightarrow {}^3T_{1g}(Cr^{4+}) + {}^3T_{2g}(Cr^{4+}) + {}^3A_{2g}(Cr^{4+})$$

$$^2D(Cr^{5+}) \rightarrow {}^2T_{2g}(Cr^{5+}) + {}^2E_g(Cr^{5+}).$$

Only in the case of Cr^{3+} ions is the ground state a non-degenerate orbital state ($^4A_{2g}$) whose spin degeneracy is removed by the spin–orbit interaction in combination with the crystalline electrical field of lower than cubic symmetry. Cr^{3+} ions ($S = 3/2$) are detectable by EPR in all phases of $BaTiO_3$.

In the three ferroelectric phases of the 3C modification the symmetry axis of the fine structure tensor is always the polar axis [12]. In contrast to Cr^{3+} the di-, tetra- and pentavalent chromium ions have doubly and triply orbital-degenerate ground states with the symmetries E, T_1 and T_2, respectively. According to the Jahn–Teller (JT) theorem such degenerate states are unstable with respect to small displacements of the neighbouring ions which lower the symmetry of the crystal field seen by the paramagnetic centre [16].

The magnetic properties of JT ions with nd^1 electron configurations were investigated in detail in $SrTiO_3$:Cr^{5+} [2–6], $SrTiO_3$:V^{4+} [17] $BaTiO_3$:Ti^{3+} [18–21] and $BaTiO_3$:Mo^{5+} [21, 22]. The prevailing tetragonal symmetry and the magnetic parameters of nd^1 ions could consistently be explained assuming a JT coupling between the $^2T_{2g}$ electronic ground state with a localized phonon mode of e symmetry in the strong coupling regime ($T_2 \otimes e$ JTE) [23]. Owing to the interaction of the phonon modes Q_θ and Q_ε (two-dimensional representation e) of the octahedral complex with the triply degenerate ground state $^2T_{2g}$ (wavefunctions xy, yz, zx), its local symmetry is reduced from cubic to tetragonal by compression along one of the three cubic axes ([100], [010], [001]). The ground state is now an orbital singlet and its energy is lowered by the JT energy [23]:

$$E_{JT} = \frac{V^2}{2\mu\omega^2} \tag{2}$$

with the effective mass μ of the phonon mode with the frequency ω. V characterizes the strength of the JT coupling. The maxima of the probability density of the unpaired 3d electron are lying in the plane perpendicular to the deformation direction. For an arbitrary orientation of the magnetic field with respect to the crystallographic axes, three EPR lines are observed in the spectrum, which are assigned to nd^1 defects with different orientations of the JT distortion. The principal values of the g tensor are [23]

$$g_\parallel = 2 - \frac{8k\lambda}{\Delta_4} \qquad \text{and} \qquad g_\perp = 2 - \frac{2k\lambda}{\Delta_1}. \tag{3}$$

The spin–orbit coupling is proportional to the constant λ being positive for one d electron. k is the orbital reduction factor and Δ_4 represents the splitting between the d_{xy} (ground state) and the $d_{x^2-y^2}$ level and can be approximated by the crystal field splitting in the cubic, undistorted precursor state. Δ_1 is the splitting of the T_2 state due to the JTE. The presence of the JTE was unambiguously proved by the behaviour of the crystals under uniaxial stress [21]. In such an experiment, the number of occupied d orbitals extending perpendicular to the stress axis increases at the cost of the others.

To explain the particularities (number of lines, directions of principal eigenvectors of g tensors) in the spectra of the Cr_I^{5+} defects in $BaTiO_3$, one must consider the special crystal structure of the low-temperature phase together with the existence of domains, in addition to the assumption of JT distortion. Shape and symmetry of unit cells and domains of ferroelectrics in thermal equilibrium are mainly determined by spontaneous deformations, which are the components S_{ik} of the symmetric deformation tensor [24]:

$$S_{ik} = \sum_{m,n} Q_{mnik} P_m^s P_n^s. \tag{4}$$

Their occurrence is the direct consequence of the existence of the spontaneous electrical polarization with the components P_m^s. The quantities Q_{mnik} are the elements of the electrostriction tensor. The deformations are quadratic in the spontaneous polarization due to the centrosymmetric high-temperature phase (paraelectric) of barium titanate. At the phase transition temperatures the vector $\vec{P}^s$ changes its direction and becomes successively oriented along the fourfold (tetragonal), twofold (orthorhombic) and threefold (rhombohedral) axes of the pseudocubic unit cell. In order that the macroscopic symmetry of a multi-domain crystal in the low-temperature phase agrees with the point group of the high-temperature one, the domains of the rhombohedral phase must be arranged according to the eight equivalent directions of the spontaneous polarization.

The spontaneous polarization is a weak perturbation and induces charge displacements in the JT-distorted $Cr^{5+}O_6^{12-}$ complex, which change the electronic wavefunctions of the Cr^{5+} ion. This polarization-induced interaction must be considered by an additional spin-Hamiltonian (5). Because the symmetry group of the JT-defect centre is D_{4h} (fourfold symmetry axis $\parallel z$) only a quadratic polarization effect is expected. The spin-Hamiltonian may be described by

$$\hat{H}^s = \sum_{i,j,k,l} T_{ijkl} P_i^s P_j^s B_k \hat{S}_l = \sum_{k,l} g_{kl}^s B_k \hat{S}_l, \tag{5}$$

where

$$g_{kl}^s = \sum_{i,j} T_{ijkl} P_i^s P_j^s \tag{6}$$

are the polarization-dependent g^s tensor components [25]. For the point symmetry D_{4h} of the defect centre the relevant fourth-rank tensor takes the form [26]

$$T_{ijkl} = \begin{pmatrix} T_{11} & T_{12} & T_{13} & & & \\ T_{12} & T_{11} & T_{13} & & & \\ T_{13} & T_{13} & T_{33} & & & \\ & & & T_{44} & & \\ & & & & T_{44} & \\ & & & & & T_{66} \end{pmatrix}. \tag{7}$$

The indices refer to the Voigt notation ($1 = xx, 2 = yy, \ldots, 6 = xy = yx$ with the pseudocubic axes x, y and z). The z axis is the tetragonal symmetry axis of the defect centre, the axis of the JT distortion. Due to the quadratic field effect, the $Cr^{5+}O_6^{12-}$ centres in domains whose polarization directions are related by inversion symmetry have the same g^s tensor. Consequently, only four differently oriented g^s tensors are generated for one special orientation of the JT distortion (z axis parallel to [001]).

In the rhombohedral phase with the spontaneous polarization along one of the ⟨111⟩ directions the axial symmetry of the g tensor of the JT-distorted $Cr^{5+}O_6^{12-}$ centres

is lifted by the elements

$$g^{s}_{xx} = g^{s}_{yy} = \frac{(P^{s})^2}{3}(T_{11} + T_{12} + T_{33})$$
$$g^{s}_{zz} = \frac{(P^{s})^2}{3}(2T_{13} + T_{33})$$
$$g^{s}_{xy} = \pm\frac{(P^{s})^2}{3}T_{66} \qquad g^{s}_{xz} = \pm\frac{(P^{s})^2}{3}T_{44} \tag{8}$$
$$g^{s}_{yz} = \pm\frac{(P^{s})^2}{3}T_{44}.$$

The four resulting g tensors have rhombic symmetry in the low-temperature phase. By spontaneous polarization the tetragonal JT splitting is marginally disturbed and the principal g values experience only small changes. A measure of the magnitude of the polarization effect is the difference between the two principal values g_2 and g_3. Due to the three possible JT distortion directions 12 g tensors are expected in a multi-domain crystal. Independently of the absolute value of the element g^{s}_{xy}, one principal axis of the 12 resulting g tensors now points in the direction of one of the equivalent ⟨110⟩ axes. The absolute values of the two other off-diagonal g tensor elements are equal and determine the angles between the $\vec{e}_3$ vectors and the ⟨001⟩ directions. Due to the very weak temperature dependence of the spontaneous polarization in the low-temperature phase, the components g^{s}_{ij} (equations (8)) are nearly temperature-independent.

Certainly, this consideration must also hold for other nd^1 ions, e.g. for Mo^{5+} ions with a $4d^1$ configuration. In this case, one likewise expects a g tensor with rhombic symmetry. Considering the angular dependence of the g values of the Mo^{5+} paramagnetic resonance spectrum ([21], figure 1), the deviation of the g tensor symmetry from the axial one is clearly visible. One principal axis of the rhombic g tensors is parallel to the equivalent ⟨110⟩ crystallographic directions. However, the very weak influence of the spontaneous polarization on the 4d wavefunction of the Mo^{5+} ion justifies the assumption of axial g tensors in the first-order explanation of the spectra. The same effects were observed in the spectra of the Ti^{3+} small polaron with the delocalized $3d^1$ electron [18].

An alternative to the $T_2 \otimes e$ JTE caused tetragonal distortion of the Cr^{5+}-surrounding oxygen octahedron is its deformation by a negatively charged Ti vacancy in a neighbouring elementary cell, which compensates for the positively charged Cr^{5+}_{Ti}. But also an off-centred position of the Cr^{5+} ion induced by a displacement along a pseudocubic axis could be the reason for a tetragonal distortion. In both cases, the local symmetry group of the Cr^{5+} defect is C_{4v} and a linear field effect is expected. Due to the lack of the inversion centre, the electrical polarizations $\vec{P}^{s}$ and $-\vec{P}^{s}$ would induce different distortions in the defect complex and two types of spectra with different principal g values should be detected in the spectra. This conclusion is contradictory to our experiments.

The difference in the temperature dependence of the single-crystal and powder spectra can be explained by the presence of internal stress in the grains of ceramics, which increases the JT energy of the $3d^1$ electron. Compared to the single crystal, the ceramic sample has a considerably higher chromium concentration, which additionally increases the stress. Thus, the transition temperature from the static to the motionally averaged JTE is increased and the Cr^{5+}_{I} spectrum of the powder samples is still detectable as spectral type b in the orthorhombic phase (figure 4). Also in this phase the Cr^{5+}_{I} spectrum must be described by a spin-Hamiltonian with rhombic symmetry on the basis of the electrical polarization along one of the ⟨110⟩ directions. Because of the distribution of the transition temperature of the rhombohedral–orthorhombic transmutation the powder spectrum at 160 K is an overlap of Cr^{5+}_{I} defect spectra in grains with rhombohedral (type a) and orthorhombic (type b) symmetry. Before all grains have adopted the orthorhombic crystal structure a motional averaging of the JT distortions sets in and a symmetric single-line spectrum with a strong temperature-dependent width is observed. Above 220 K, this line is not detectable due to its greatly increased linewidth.

5. Conclusions

The paramagnetic ion Cr^{5+} with the electron configuration $3d^1$, incorporated into the perovskite lattice on the B site (Ti site), shows also in barium titanate a $T_2 \otimes e$ Jahn–Teller effect. Due to the existence of a spontaneous electrical polarization, present in all ferroelectric phases of $BaTiO_3$, the tetragonal Jahn–Teller distortion of the $Cr^{5+}O_6^{12-}$ complex is weakly disturbed by a quadratic field effect and the D_{4h} symmetry of the complex is reduced. EPR spectra with rhombic symmetry are detected in the rhombohedral (spectral type a) and orthorhombic (spectral type b) phases and are assigned to the Cr^{5+}_{I} defect. The abnormal position of the principal axes of the g tensor for the spectral type a can be accounted for in this polarization model. Because the three equivalent axes of the tetragonal JT distortions occur in each of the ferroelectric domains, the number of non-equivalent g tensors is dictated by the domain structure of the $BaTiO_3$ crystal.

Acknowledgments

The authors thank Professor O F Schirmer (Universität Osnabrück) for providing the single crystal, very helpful discussions and critical reading of the manuscript, and Mrs U Heinich and Dipl.-Ing. J Hoentsch for help in the measurements of the EPR spectra.

References

[1] Possenriede E, Schirmer O F, Albers J and Godefroy C 1990 *Ferroelectrics* **107** 313
Possenriede E, Jacobs P and Schirmer O F 1992 *J. Phys.: Condens. Matter* **4** 4719
Possenriede E 1992 *PhD Thesis* University of Osnabrück
[2] Lagendijk A, Morel R J, Glasbeek M and van Voorst J D W 1972 *Chem. Phys. Lett.* **12** 518

[3] de Jong H J and Glasbeek M 1978 *Solid State Commun.* **28** 683
[4] de Jong H J and Glasbeek M 1976 *Solid State Commun.* **19** 1197
[5] Müller K A, Blazey K W and Kool Th W 1993 *Solid State Commun.* **85** 381
[6] Kool Th W, de Jong H J and Glasbeek M 1994 *J. Phys.: Condens. Matter* **6** 1571
[7] Langhammer H T, Müller T, Felgner K-H and Abicht H-P 2000 *J. Am. Ceram. Soc.* **83** 605
[8] Langhammer H T, Müller T, Böttcher R and Abicht H-P 2003 *Solid State Sci.* **5** 965
[9] Böttcher R, Erdem E, Langhammer H T, Müller T and Abicht H-P 2005 *J. Phys.: Condens. Matter* **17** 2763
[10] Langhammer H T, Müller T, Böttcher R and Abicht H-P 2008 *J. Phys.: Condens. Matter* **20** 085206
[11] Böttcher R, Langhammer H T, Müller T and Abicht H-P 2008 *J. Phys.: Condens. Matter* **20** 505209
[12] Müller K A, Berlinger W and Albers J 1985 *Phys. Rev.* B **32** 5837
[13] Stoll St 2003 Spectral simulation in solid-state EPR *PhD Thesis* ETH Zürich
[14] Schonland D S 1959 *Proc. Phys. Soc. Lond.* **73** 788
[15] Schläfer H L and Gliemann G 1967 *Einführung in die Ligandenfeldtheorie* (Leipzig: Geest and Portig)
[16] Abragam A and Bleaney B 1970 *Electron Paramagnetic Resonance of Transition Metal Ions* (Oxford: Clarendon)
[17] Kool Th W and Glasbeek M 1979 *Solid State Commun.* **32** 1099
Kool Th W and Glasbeek M 1991 *J. Phys.: Condens. Matter* **3** 9747
[18] Scharfschwerdt R, Mazur A, Schirmer O F, Hesse H and Mendricks S 1996 *Phys. Rev.* B **54** 15284
[19] Lenjer S 1999 *PhD Thesis* University of Osnabrück
[20] Schirmer O F, Kool Th W, Lenjer S and Maiwald M 2005 *Phys. Status Solidi* c **2** 124
[21] Lenjer S, Schirmer O F, Hesse H and Kool Th W 2002 *Phys. Rev.* B **66** 165106
[22] Schwartz R W, Wechsler A B and West L 1995 *Appl. Phys. Lett.* **67** 1352
[23] Ham F S 1972 *Electron Paramagnetic Resonance* ed S Geschwind (New York: Plenum)
[24] Strukov B A and Levanyuk A P 1998 *Ferroelectric Phenomena in Crystals: Physical Foundations* (Berlin: Springer)
[25] Pake G E and Estle T E 1973 *The Physical Principles of Electron Paramagnetic Resonance* (Cambridge, MA: Benjamin)
[26] Haussühl S 2007 *Physical Properties of Crystals: an Introduction* (Weinheim: Wiley/VCH)